Quarterly Progress Report

For Period

January 1 to March 31, 1968

FUNDAMENTAL STUDIES OF THE METALLURGICAL, ELECTRICAL, AND OPTICAL PROPERTIES OF GALLIUM PHOSPHIDE

Grant No. NsG-555

Prepared For

NATIONAL AERONAUTICS AND SPACE ADMINISTRATION
LEWIS RESEARCH CENTER
CLEVELAND, OHIO

Work Performed By

Solid-State Electronics Laboratories
Stanford University
Stanford, California

PROJECT 5112: THE PROPERTIES OF RECTIFYING JUNCTIONS IN $GaAs_xP_{1-x}$

National Aeronautics and Space Administration
Grant NsG-555
Project Leader: G. L. Pearson
Staff: S. F. Nygren

The purpose of this project is to study the preparation and characterization of rectifying junctions in GaP and $GaAs_xP_{1-x}$. In particular, we wish to relate the structure of the crystals to the electrical properties of the p-n junctions. During this quarter, we have formed p-n junctions by the diffusion of zinc into n-type gallium phosphide under high phosphorus pressures. The relationship among junction depth, temperature, and phosphorus pressure has been determined. Junctions have also been formed by growing beryllium-doped liquid epitaxial layers of gallium phosphide on n-type gallium phosphide seeds. It was found that a layer with a hole density of 8.7×10^{18} cm^{-3} can be grown from a gallium solution containing 1.4×10^{-2} atom per cent beryllium.

A. Diffusion of Zinc into Gallium Phosphide

L. L. Chang[1] has shown that if the zinc diffusion coefficient is a function of only the zinc concentration, and if the diffusion profile is sufficiently steep-fronted, then the junction depth, x_j, should obey

$$x_j = A \sqrt{\bar{D}_o t} \quad , \tag{1}$$

where A = constant for a given temperature, $\bar{D}_o$ = diffusion coefficient at the surface, t = time.

We have checked this relationship at 800^oC and 900^oC using a pure zinc diffusion source. This source places the system in monovariant region #1 of the phase diagram, as described in the previous report.[2]

Liquid "a" is present in the system. The results of these diffusions, plotted in Fig. 1, show significant variations from the predicted dependence on t. For comparison, Fig. 1 also includes data from diffusions done with excess phosphorus - 2.2 atmospheres of P_4. The system contained only solid GaP, solid Zn_3P_2, and a vapor phase - no liquids. It is seen that the junction depth is proportional to $\sqrt{t}$ when the phosphorus pressure is high.

In order to examine the properties of diffusions done in monovariant region #2 of the phase diagram, it was first necessary to calculate the vapor pressures that exist over the Ga-P-Zn liquidus. No experimental results are available. The pressures were calculated by applying the regular solution method of Furukawa and Thurmond[3] to extrapolations of Panish's[4] phase diagram. The results for the pressures of P_4 and Zn , the dominant species in region #2, are shown in Fig. 2.

Diffusions were done in region #2 using 0.21 cm^3 ampoules, each containing a GaP sample, excess GaP powder, 0.87 mg Ga, 2.72 mg P, and 3.41 mg Zn. The diffusion source was chosen to provide the proper condensed phases and vapor pressures for region #2, even if the pressure calculations were in error by ± 50%. Diffusions using different amounts of excess phosphorus at 900°C demonstrated that the above source is correct for 900°C, and, presumably, is correct from 750°C to 1000°C.

The p-n junctions were revealed by our usual cross-sectioning and etching procedure. The results of diffusions with liquid "b" are similar to those with liquid "a" in that precipitation and diffusion

induced defects are evident, particularly above 900°C. However, there are two major differences between diffusions done with the two different liquids. For a given temperature and time, a p-n junction formed by diffusion with liquid "b" in the system is shallower and more planar than one formed with liquid "a". This is shown in Fig. 3 where the minimum junction depth (labeled "front") and the average depth of a diffusion spike found at a stacking fault are plotted against reciprocal temperature.

These results may be explained qualitatively. Equilibrium relationships may be used to calculate C_s^o, the surface concentration of zinc:

$$C_s^o = \left(\frac{P_{Zn} P_{P_4}^{1/4}}{k_s \gamma_p} \right)^{1/2}, \tag{2}$$

where P_{Zn} and P_{P_4} are the pressures of Zn and P_4, k_s is constant for a given temperature, and γ_p is the hole activity coefficient. The diffusion coefficient may be calculated from the interstitial-substitutional model:

$$\bar{D} = \left(2 + \frac{C_s}{\gamma_p} \frac{d\gamma_p}{dC_s}\right)\left(k_1 D_i \gamma_p^2 C_s^2 P_{P_4}^{-1/4}\right) + \left(2 + \frac{C_s}{\gamma_p} \frac{d\gamma_p}{dC_s}\right)\left(k_2 P_{P_4}^{1/4}\right) \text{ if } n = 1 \tag{3}$$

$$\bar{D} = \underbrace{\left(3 + \frac{2C_s}{\gamma_p} \frac{d\gamma_p}{dC_s}\right)\left(k_1 D_i \gamma_p^3 C_s^3 P_{P_4}^{-1/4}\right)}_{\text{interstitial}} + \underbrace{\left(2 + \frac{C_s}{\gamma_p} \frac{d\gamma_p}{dC_s}\right)\left(k_2 P_{P_4}^{1/4}\right)}_{\text{substitutional}} \text{ if } n = 2 \tag{4}$$

where $\bar{D}$ = effective diffusion coefficient, D_i = interstitial zinc diffusion coefficient, C_s = zinc concentration, k_1 and k_2 = constants at a given temperature, + n = charge state of interstitital zinc;

n = 1 or 2, but it is disputed in the literature.

By using Eq. (2) Panish and Casey's[5] data for the hole activity coefficient, and Chang and Pearson's[6] data for zinc surface concentration with liquid "a", the surface concentration for liquid "b" may be calculated. Likewise, by using Eqs. (1) and (2) and either (3) or (4), and by assuming the interstitital term dominant at all pressures, the junction depth for liquid "b" may be calculated from the junction depth for liquid "a". The experimental and calculated results are shown in Fig. 4. It is seen that the calculated results for junction depth do not agree exactly with the experimental results. This is not surprising, given the crudeness of the pressure calculations and the violation of Eq. (1) by diffusions from liquid "a". However, the calculations do show that a shallower diffusion with liquid "b" is expected.

Equations (3) and (4) also demonstrate why the diffusion front with liquid "b" is more planar than with liquid "a". Chang and Pearson[7] have demonstrated that the diffusion coefficient is strongly concentration dependent when liquid "a" is present. In this case the interstitital term dominates, and an inhomogeneity in a sample that changes the zinc concentration will also change the diffusion coefficient, making the diffusion front irregular. As phosphorus pressure is increased, the interstitital term decreases, and the substitutional term increases. Apparently, with liquid "b" the two terms approach the same order of magnitude, making the diffusion coefficient considerably less concentration dependent. That, coupled with the fact that the increased phosphorus pressure probably leads to a more homogeneous

crystal, leads to a considerably more planar diffusion front.

B. Liquid Epitaxy

We have begun to grow liquid epitaxial layers of GaP doped with Be. Our initial series of runs yielded only one good layer. It was grown by our standard technique: A 93 μg chip of Be, 4.99 g of Ga, and enough GaP to more than saturate the Ga at 960°C was loaded into the source end of the boat. The source was heated from room temperature to 950°C in 60 minutes and allowed to stabilize for 15 minutes. Then it was brought into contact with the seed and cooled at 0.375°/min until 660°C was reached. At that point, the furnace was shut off. In the temperature range from 950°C to 660°C, the solubility of GaP in Ga decreases from 1.5 a/o (atom per cent) to 2.3×10^{-2} a/o [8] so that 98% of the crystal is grown, and the solubility of Be in Ga decreases from 3.4 a/o to 4.2×10^{-1} a/o [9]. If the 93 μg Be dissolved completely in the 4.99 g Ga, the concentration would be 1.4×10^{-2} a/o.

The Be-doped layer was p-type, and the diode formed by the layer and the n-type substrate gave off green electroluminescent light. The layer was heavily doped, and gold dots evaporated onto it formed ohmic contacts without being alloyed. A Van der Pauw sample was made from an 89 μ thick slab taken from the layer. Neglecting possible variations in doping concentration as a function of depth within the layer, we measured $p = 8.7 \times 10^{18}$ cm^{-3} (1.75×10^{-2} a/o) and $\mu_H = 34$ cm^2/v sec at room temperature. At 80°k, the measurements were $p = 8.7 \times 10^{18}$ cm^3 and $\mu_H = 18$ cm^2/v sec.

The Be-doped layer was unusual in many respects. First, the layer was much thicker than normal: 180 μ as compared to 60-90 μ

usually found with undoped layers. Second, about 30 μ of the seed had been melted before the layer began to grow, compared with no melt-back at all with undoped or zinc-doped layers. Third, the Be had diffused about 20 μ into the seed from the seed/layer interface, compared with no measurable diffusion seen in layers doped to 10^{17} cm^{-3} with zinc.

Attempts to grow a Be-doped layer from a solution containing 2.1×10^{-1} a/o Be resulted in severe melt-back and crystal regrowth in only a few isolated islands. This is not surprising since a Be density of 10^{19} cm^{-3} is probably very close to the solubility of Be in GaP at 950°C. At 930°C, the solubility of Be in GaAs, a material similar to GaP, is about 2×10^{19} cm^{-3} .[10] In the future we shall attempt to grow layers that are more lightly doped with Be.

REFERENCES

1. L. L. Chang, Solid State Electronics, 7, 853 (1964).
2. S. F. Nygren, Quarterly Progress Report, September 30 to December 31, 1967.
3. Y. Furukawa and C. D. Thurmond, J. Phys. Chem. Solids, 26, 1534 (1965).
4. M. B. Panish, J. Electrochem. Soc., 113, 224 (1966).
5. M. B. Panish and H. C. Casey, Jr., Bull. Am. Phys. Soc., 13, 375 (1968).
6. L. L. Chang and G. L. Pearson, J. Phys. Chem. Solids, 25, 23 (1964).
7. L. L. Chang and G. L. Pearson, J. Appl. Phys., 35, 1960 (1964).
8. R. N. Hall, J. Electrochem. Soc., 110, 385 (1963).
9. Reed O. Elliot and Eugene M. Cromer, U. S. Atom. Energy Comm. AECU-3022 (1952).
10. E. A. Poltoratskii and V. M. Stuchebnikov, Sov. Phys.-Sol. St., 8, 770 (1966).

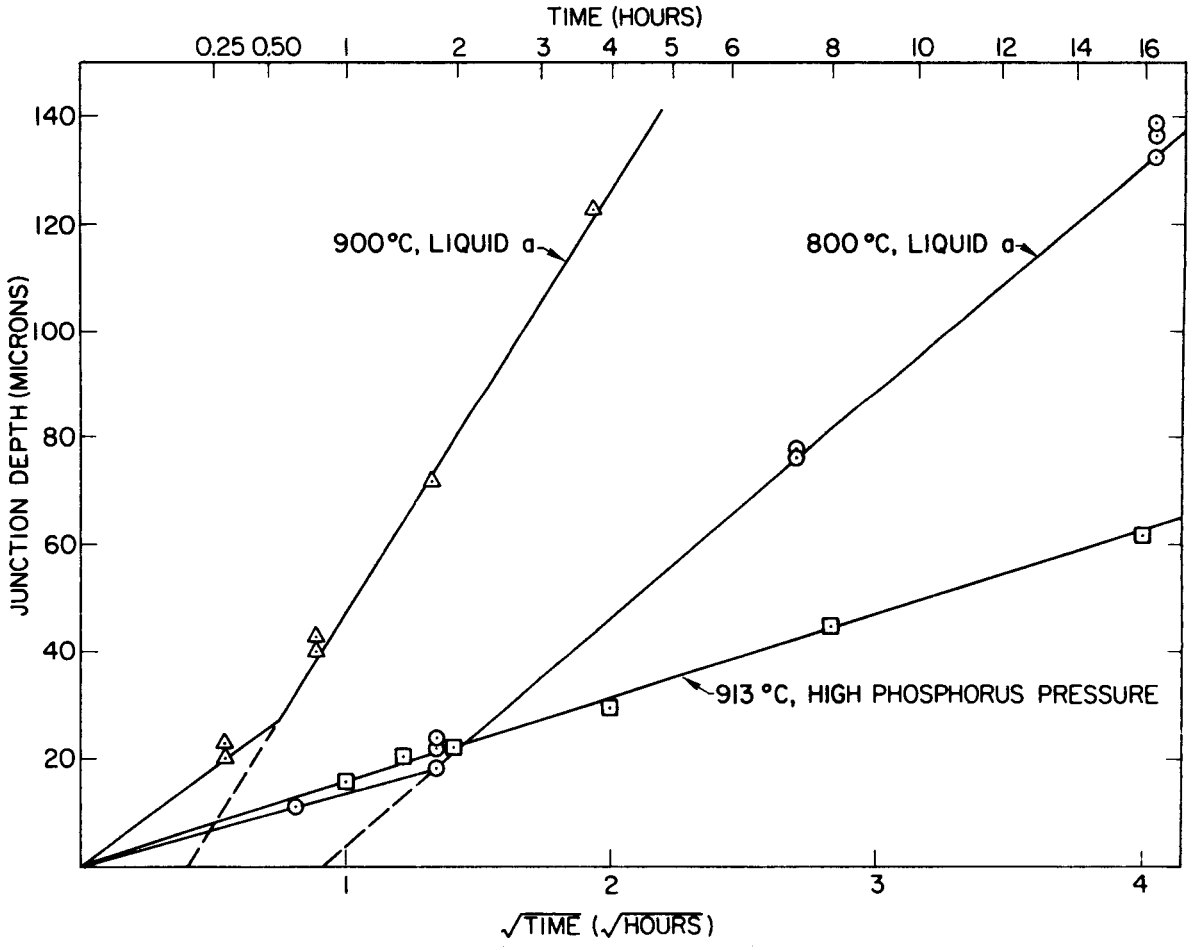

FIG. 1 - Minimum p-n junction depth vs. square root of time for diffusions from liquid "a" at 800°C and 900°C, and for diffusions from high phosphorus pressure at 912°C.

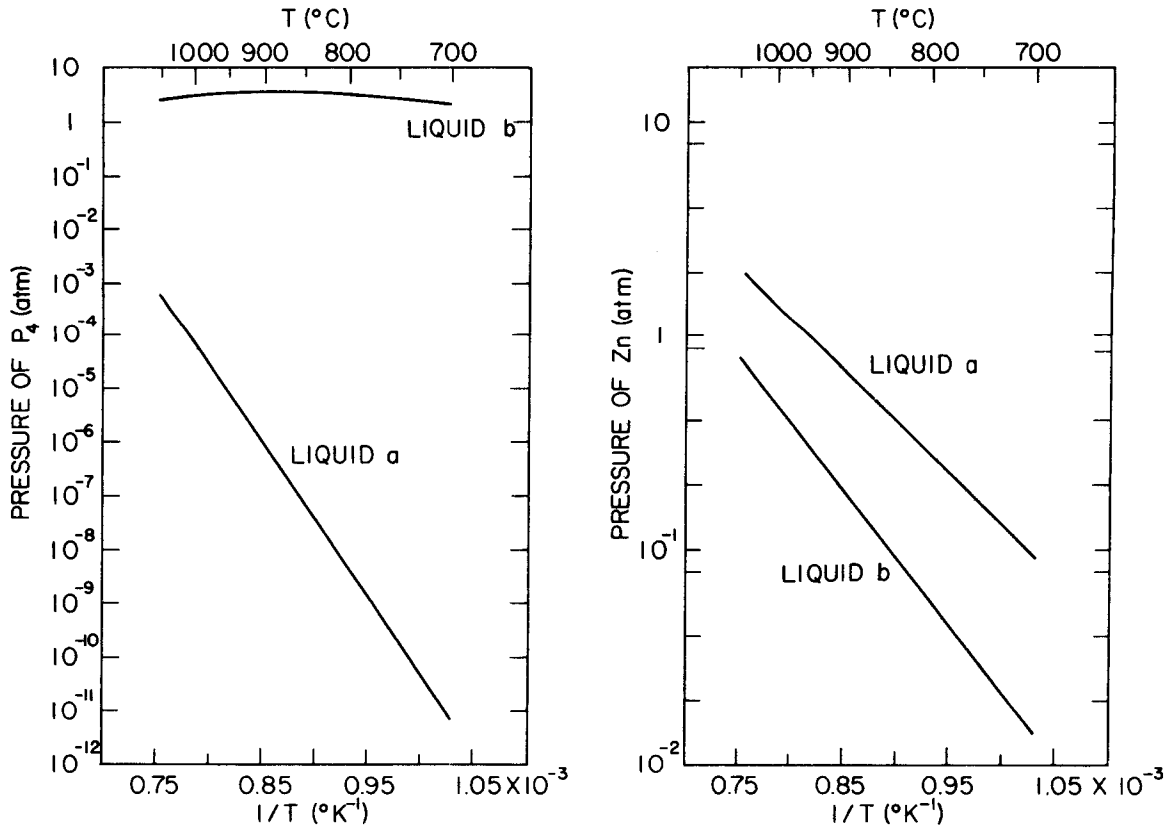

FIG. 2 - The pressures of P_4 and Zn over liquids "a" and "b" between 700°C and 1050°C.

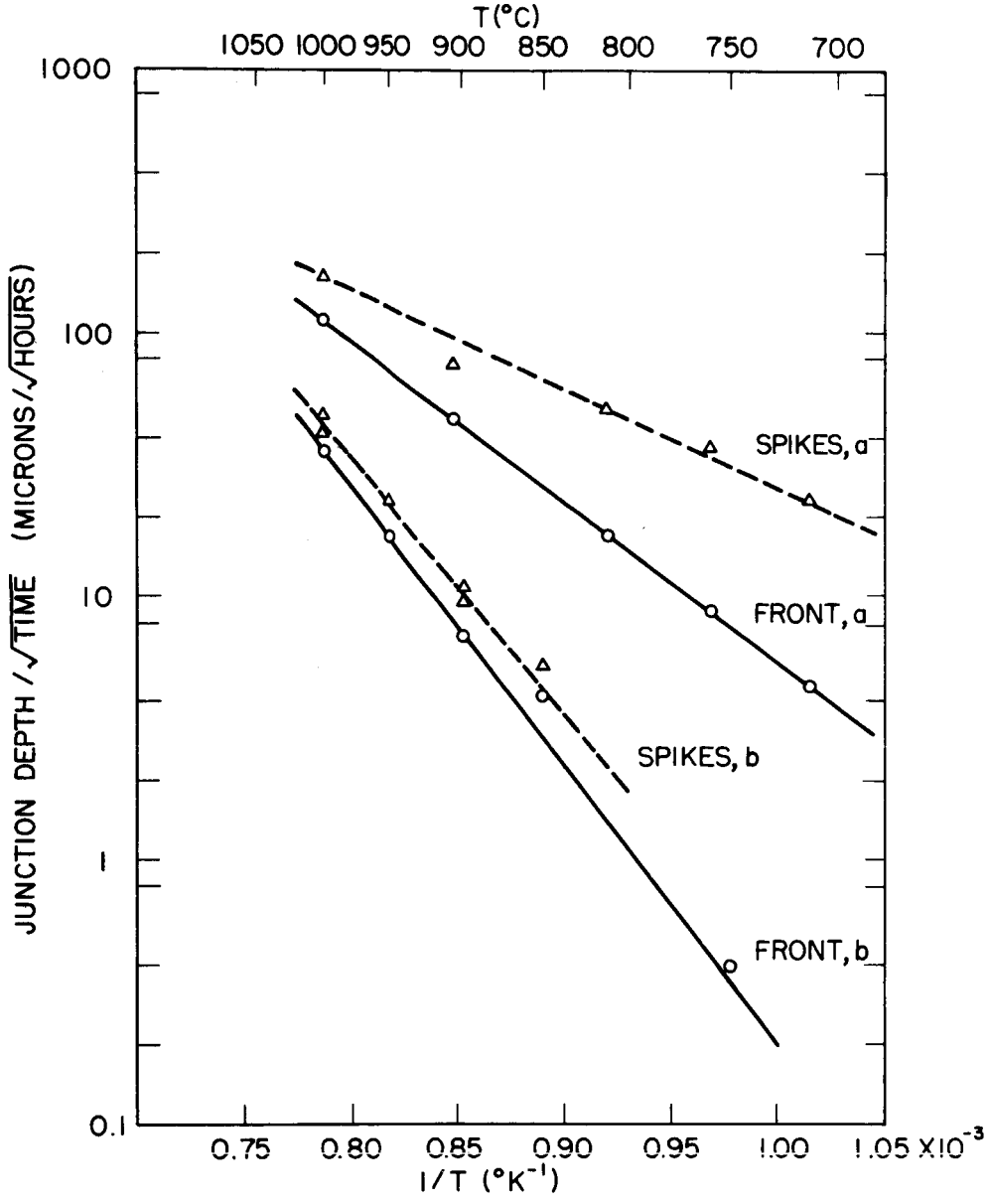

FIG. 3 - Minimum p-n junction depth and average spike depth normalized to one hour vs. reciprocal temperature.

B43598

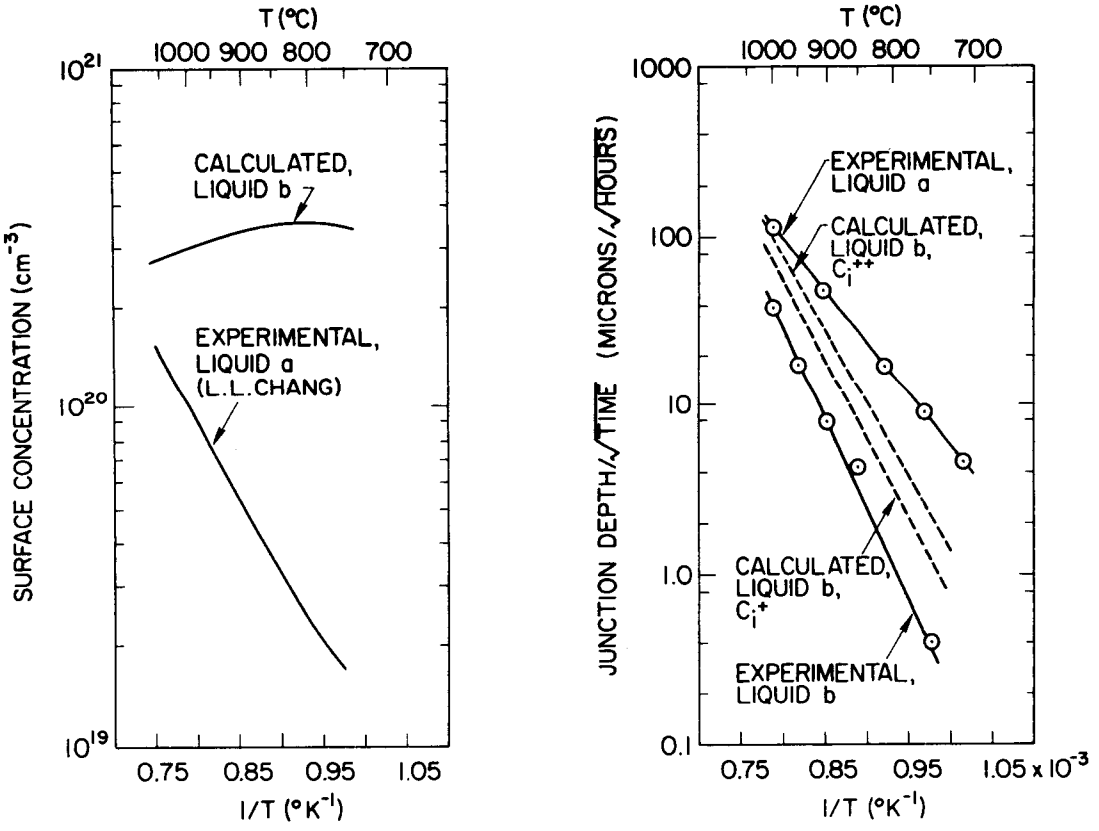

FIG. 4 - Surface concentration and p-n junction depth vs. reciprocal temperature for diffusions done with liquid "a" or liquid "b".

B49085

PROJECT 5115: SEMICONDUCTOR DEVICES FOR HIGH TEMPERATURE USE

National Aeronautics and Space Administration
Grant NsG-555
Project Leader: G. L. Pearson
Staff: Y. Nannichi

The purpose of this project is to prepare power rectifiers and solar batteries which will operate at temperatures up to 500°C. Previous experiments showed the feasibility of Ni: n-GaP Schottky diodes as power rectifiers. The main effort this month was concentrated on increasing the reverse breakdown voltage as well as decreasing the forward resistance of these devices.

A. Vapor-epitaxial crystals

Seven crystals were grown by vapor epitaxy. Typical growth conditions were: H_2 flow rate. 110 cm^3/min (main) and 45 cm^3/min (PCl_3 bubbler at 0°C); temperature of Ga boat, ~ 930°C, temperature of GaAs substrate, 860°C (vapor etch for 5 min) and 820°C (growth).

The properties of these crystals are shown in Table 1. The impurity concentrations of the undoped crystals were in the range of $10^{15} \sim 10^{16}$ cm^{-3}. PCl_3 from a new bottle seemed to give somewhat higher electron concentrations in the grown crystals, though the old and the new bottles bore the same lot number.

It was tried once (VG-2) to grow a p-type crystal by using 0.1 wt % solution of CdI_2 in PCl_3, but it seemed that cadmium was not transported at all. No further attempt was made to incorporate impurities in vapor grown epitaxial crystals.

A new setup for growing heterojunctions was completed. Two independent Ga boats are for $AsCl_3$ and PCl_3 respectively, and the

positions of the boats are adjustable so as to control the temperatures.

B. Liquid-epitaxial crystals

Five undoped crystals were grown by liquid epitaxy from Ga on substrates grown by vapor epitaxy. As shown in Table 2 the electron concentrations of these undoped liquid-epitaxial crystals were comparable to those of vapor-epitaxial crystals. Originally the purpose of growing liquid epitaxial crystals on vapor epitaxy crystals was to get crystals with more uniformity and fewer crystal imperfections. A comparison of these two methods is shown in Fig. 1, in which the breakdown voltages of Schottky barriers versus electron concentrations are plotted.

Two crystals were grown from Ga containing 0.6 mol % Sn. The crystals contained $\sim 10^{17}$ cm^{-3} net donors, which gives the distribution coefficient of Sn, $\sim 10^{-4}$. This value is in good agreement with that given by Trumbore et al[1] at 1070°C in GaP as well as that obtained by J. Harris[2] in GaAs. The variation of electron concentration was within 50% in the first 50 μ. The growth temperature was 950°C at the interface and 820°C after growing 50 μ so the distribution coefficient seems to be only a weak function of temperature from 820 to 1070°C.

C. V-I Characteristics of Schottky diodes at room temperature

Due to the tendency to cleave in (110) planes, which is inherent to most III-V compounds, it is extremely difficult to lap GaP crystals thinner than 50 μ. On the other hand, only 10 μ are necessary to obtain breakdown voltage of 100 V, which is our tentative goal. LG8 and LG9 were grown in trials to reduce the forward series resistance. Liquid epitaxial crystals of about 60 μ thickness, containing 10^{17} Sn/cm^3, were grown on the B plane of crystal VG 6 which was 200 μ thick.

Schottky diodes were made on the VG6 side after reducing the total thickness to 175 μ. The structure of the diode is shown in the inset of Fig. 2. Figure 2 also shows the static forward V-I characteristics of the Schottky diode. The forward current is approximated by the following equation:

$$I \simeq I_o \exp(\frac{eV}{nkT}) \ .$$

The slope of the curve, n, is 1.75 for $0 \leq V < 0.5$ volts and 1.5 for $0.5 < V < 1$ volts. I_o was extrapolated from the region $0.5 < V < 1$, to be about 2×10^{-17} A($\simeq 1.7 \times 10^{-14}$ A/cm^2). Departures from the ideal case (n = 1.0) is usually attributed to the surface treatment.[3] In the present case, the polished surface was slightly etched with the solution [$8K_3Fe(CN)_6$: 12KOH: $100H_20$] just prior to the evaporation of Ni.

The forward differential resistance was about 200Ω, and this will be reduced in the future. The dc reverse characteristics are shown in Fig. 3. A hysteresis is clearly seen at the breakdown. On the Tektronix curve tracer more complicated breakdown curves were observed (Fig. 4). Though we have not studied this phenomenon carefully, it is probably due to the slow states which we reported in the previous quarterly report.

D. Observation of microplasmas

We observed microplasmas through semi-transparent Ni or Au films in reverse-biased diodes. There were three types of patterns; i.e., i) spot, ii) line and iii) edge.

Spot luminescence was often seen in vapor-epitaxial crystals (Fig. 5a). Line luminescence (Fig. 5b) was seen only in liquid epitaxial crystals. The spots developed into lines in increasing the current which resembled the evolution of the near field pattern in semiconductor junction lasers. The lines were parallel to one of the (110) axes and their lengths reached 15 μ. Line luminescence could be caused by the accumulation of impurities which was due to the repeating cycle of super saturation and growth. We were unable to find a correlation between the etch pattern and the luminescence pattern because of inadequate etching.

Edge luminescence (Fig. 5c) is due to a concentration of the electric field.[4] This type of breakdown could be avoided in a mesa or a guard ring structure.

The knicks in the reverse characteristics (a and b in Fig. 4b) are due to these microplasmas.

E. Plans for the next quarter.

GaP crystals will be grown from Sn solutions to get more heavily doped crystals. Heterojunctions will also be grown by vapor epitaxy which will serve as photocells and ohmic contacts. Ion bombardment will be tried in an attempt to obtain a clean interface at the Schottky barrier.

Techniques of mesa etching will be pursued to reduce the surface leakage current as well as to eliminate the edge breakdown.

V-I characteristics will be studied at higher temperatures in various gas ambients.

REFERENCES

1. F. A. Trumbore, et al., J. Electrochem. Soc., 112, 1208 (1965).

2. J. Harris, Quarterly Progress Report, Project K702, December 1967.

3. M. Lepselter and S. Sze, Bell System Technical Journ., 195 (1968).

4. S. Sze and G. Gibbons, Solid State Electronics, 9 831 (1966).

TABLE 1. Properties of Vapor-Epitaxial Crystals

Sample Number	Growth Time (min)/Thickness (μ)	Electron Concentration (cm^{-3})	Breakdown Voltage (V)	Remarks
VG 2	220/220	$3 \sim 6 \times 10^{15}$	15	CdI_2 doped in bubbler
VG 3	300/200	$5 \sim 14 \times 10^{15}$	10	
VG 4	445/350	$1 \sim 3 \times 10^{15}$	~50	
VG 5	540/500	4.4×10^{15}	15	Extremely smooth surface
VG 6	340/400	1×10^{16}	42	New bottle of PCl_3
VG 7	540/450	1×10^{16}	20	Pyramids on the surface

TABLE 2. Properties of Liquid-Epitaxial Crystals

Sample Number	Growth Time (hr)/Thickness (μ)	Substrate	Electron Concentrations (cm^{-3})	Breakdown Voltage(V)	Remarks
LG 2	18/80	VG-4	3×10^{16}	3	
LG 3	18/60	VG-7A	1×10^{16}	10	
LG 4	18/97	VG-7A	$.4 \sim 1.5 \times 10^{16}$	80	
LG 5	18/90	VG-7A	1×10^{16}	100	
LG 6	18/78	VG-7A	4×10^{15}	60	
LG 8	18/70	VG-6	6×10^{16}	~ 8	Sn-doped
LG 9	18/60	VG-6	1×10^{17}	~ 10	Sn-doped

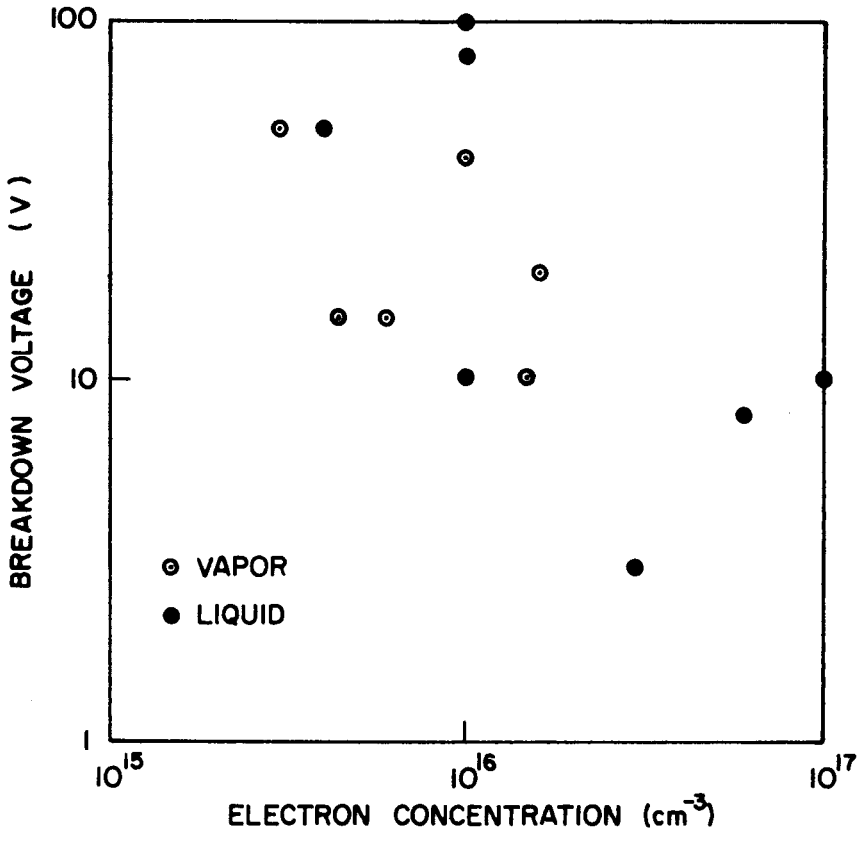

FIG. 1 - Breakdown voltage vs. electron concentrations of vapor and liquid epitaxial crystals.

A44073

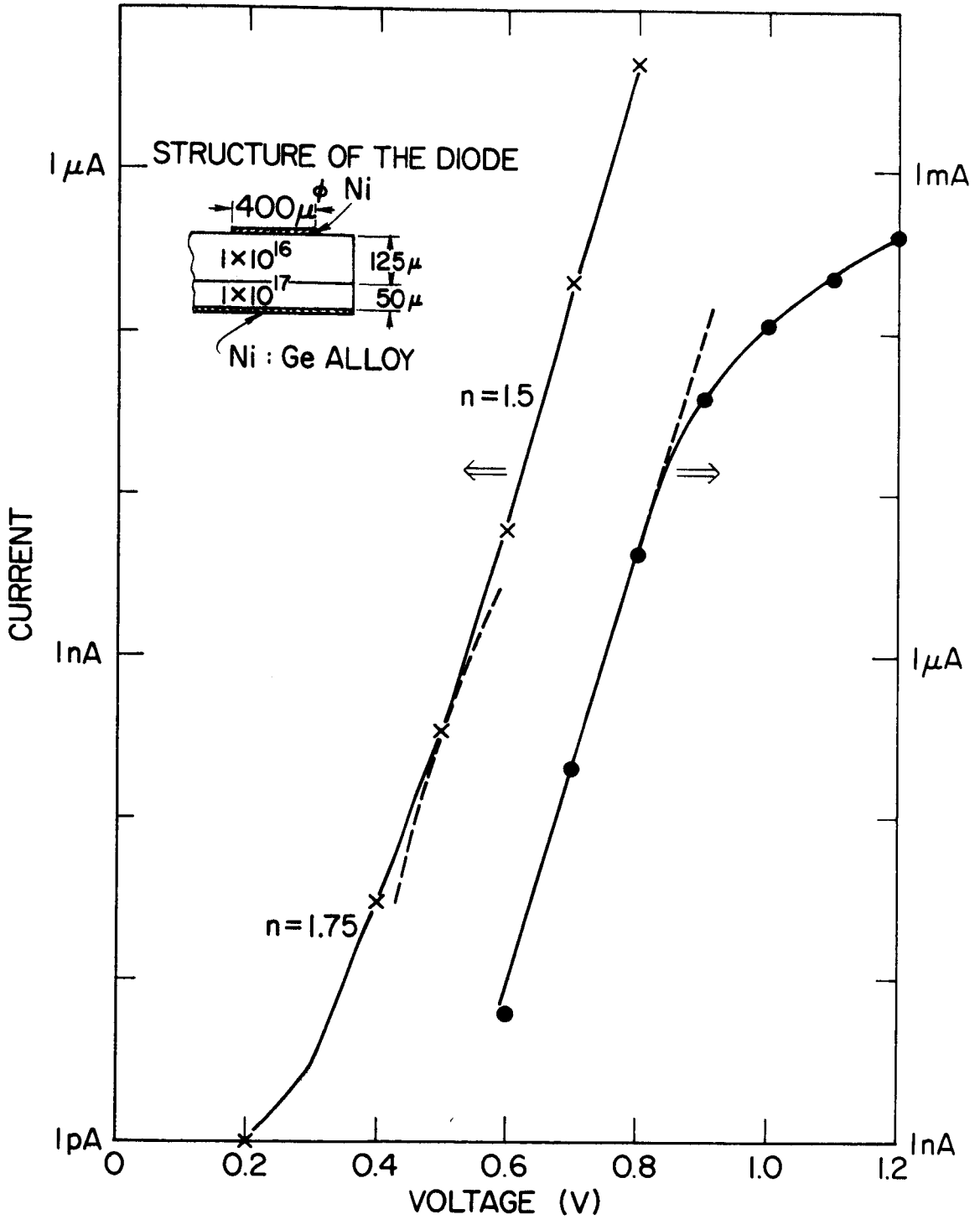

FIG. 2 - Forward characteristics of a GaP Schottky diode.

B44074

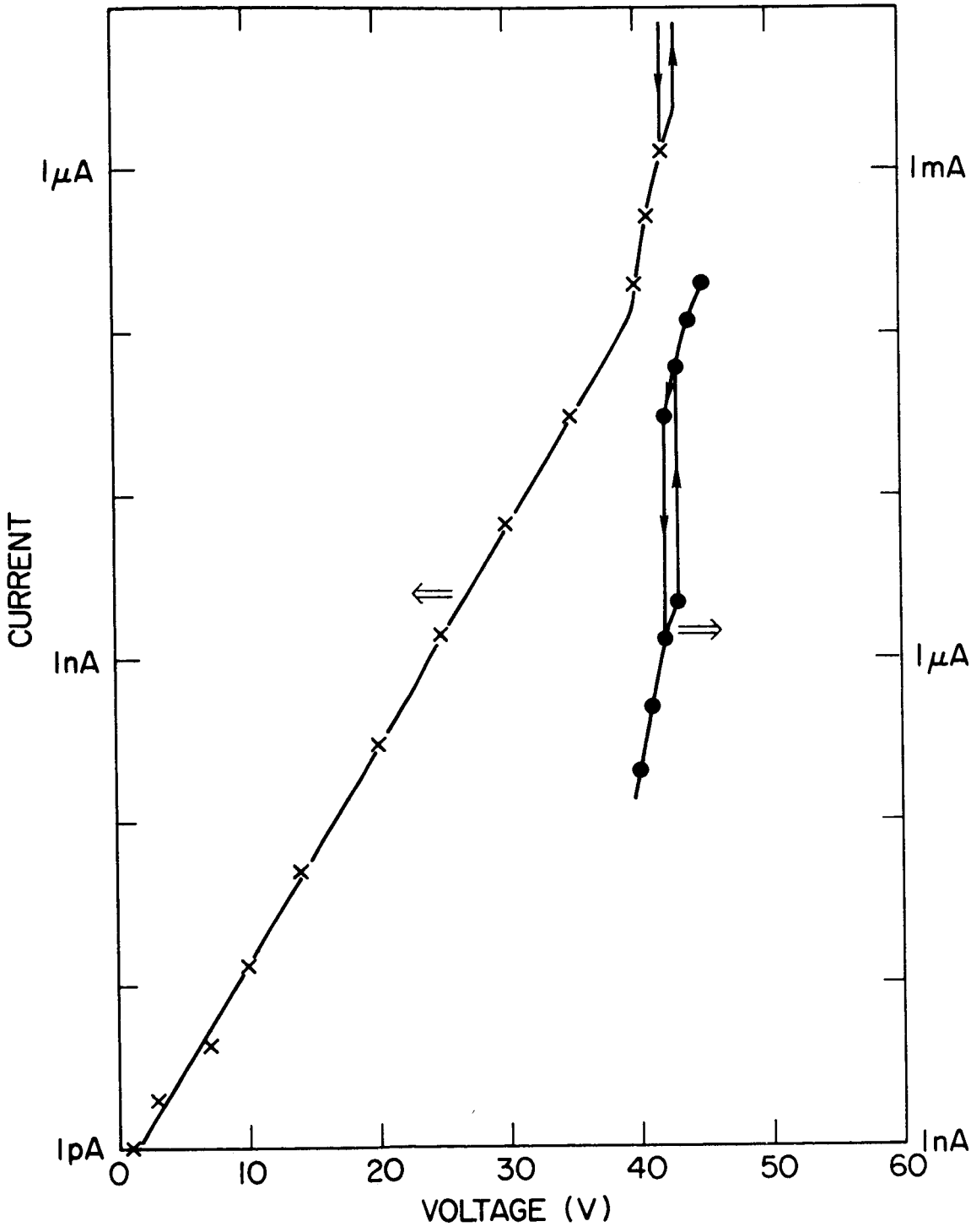

FIG. 3 - Reverse characteristics of a GaP Schottky diode.

B44075

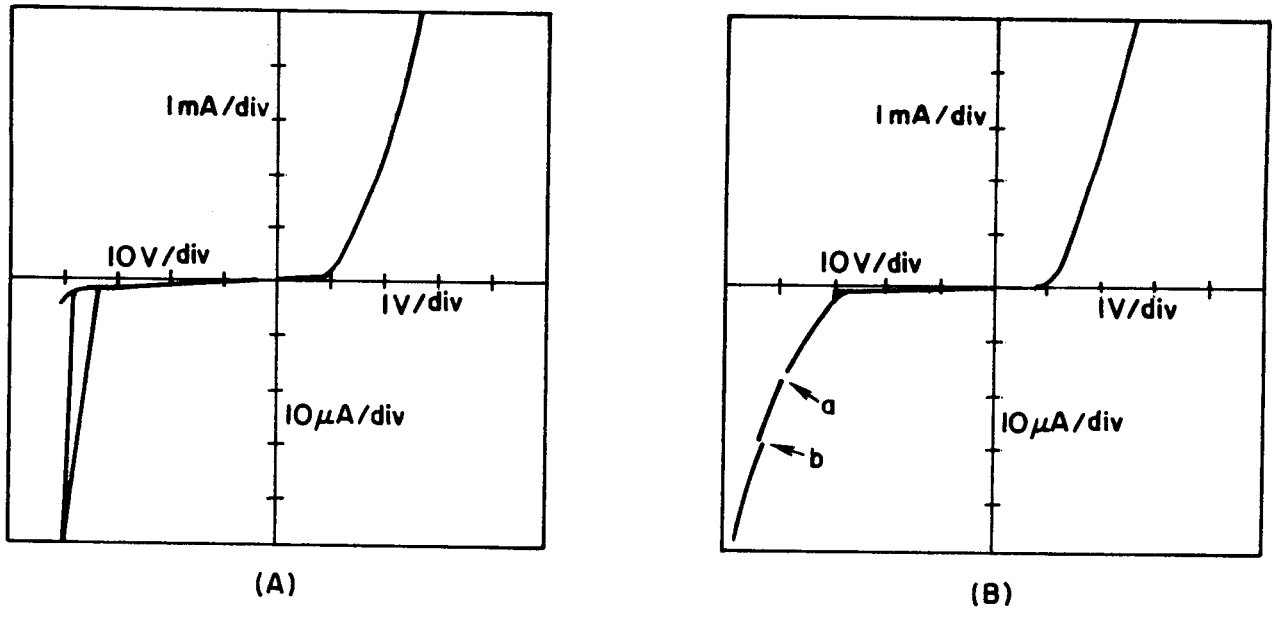

FIG. 4 - Characteristics on Curve Tracer.

A44076

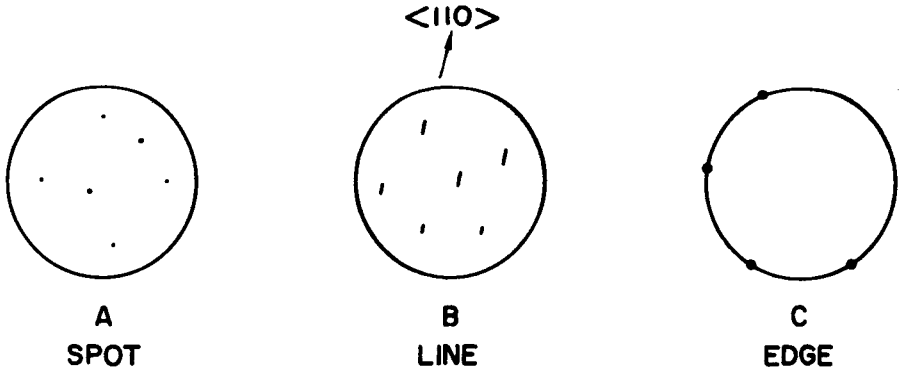

FIG. 5 - Patterns of luminescence.

PROJECT 5116: DONOR IMPURITIES IN GaP

National Aeronautics and Space Administration
Grant NsG-555
Principal Investigator: G. L. Pearson
Staff: A. Young*

The purpose of this project is to study the behavior of shallow donors in gallium phosphide. In particular S, Se, and Te will be diffused into GaP to determine solubility and diffusion parameters. This information will be useful in delineating the properties of GaP doped with these shallow donor impurities.

Diffusion of Sulfur Through Silicon Oxide Film

A 2200Å SiO_2 film was deposited onto a GaP sample with an r-f. glow discharge system using silane and nitrous oxide. The film was then annealed at 600°C for 4 hours in a nitrogen atmosphere to improve its adherence and density. 20 micrograms of non-radioactive sulfur was placed in an ampoule with the sample and diffused for 12 hours at 1215°C. No excess phosphorus was used. Although some cracking of the film and a few pinholes developed during the diffusion, the surfaces in general were quite good. (Film depositions on heated substrates are expected to be even better.)

Incremental Hall measurements were made on the "b" face to determine the carrier concentration as a function of depth. The results are shown in Fig. 1. Unfortunately, no radiotracer profile is available for this sample. However, previous results indicate that the diffusion fronts determined by radiotracer and Hall measurements should coincide fairly well. The presence of the film has reduced the effective junction depth to 6 microns - without the film, the junction depth would be expected to be about 15 microns. This result implies that

* NSF Fellow

the diffusion coefficient of sulfur in GaP is perhaps 3 orders of magnitude larger than in SiO_2, and suggests that depletion of the vapor source by diffusion into the quartz ampoule should not be a serious problem.

In order to check that the diffused layer was doped with sulfur, and not with silicon (from the SiO_2 film) a control sample of SiO_2 film on GaP was heated in the absence of sulfur for 12 hours at 1215°C. Hall measurements indicate that the sample after heat treatment was p-type with a carrier concentration in the 10^{14} cm^{-3} range. Further study would be needed to determine if the acceptor is copper, silicon on a phosphorus site, or something else.

These SiO_2 films will be used in incremental Hall measurements on diffused layers to eliminate uncertainties due to rough surfaces.

Hall Measurements on Sulfur-Diffused Layer (77°K to 500°K)

A sample diffused with sulfur through a 2200Å SiO_2 film was mounted on a transistor header and Hall measurements were made from 77°K to 500°K. Assuming a homogeneous layer of thickness 6 microns as determined by incremental sheet resistivity measurements on the opposite face, average carrier concentration, mobility, and resistivity of the layer were determined as a function of temperature. The results are shown in Fig. 2.

The apparent minima in the electron concentration and maximum in the mobility have been observed previously by other experimenters[1] and attributed to the onset of impurity-band conduction. For $n > 1\text{-}2 \times 10^{18}$ cm^{-3}, a metallic form of impurity band conduction is believed to exist, leading to electrical parameters that are only weakly dependent on temperature.

In the high temperature region, the mobility can be fit well with a combination of polar lattice scattering and space-charge scattering (with $N_s A = 10^3$).[2]

At room temperature the average carrier concentration is 5×10^{18} cm^{-3} and increases to 9×10^{18} cm^{-3} at $500^{o}k$ with no evidence of a saturation region. It would be of some interest to extend measurements to higher temperatures.

An activation energy of about 0.060 eV (2 X 0.030) is deduced from the straight line portion of the electron concentration curve in reasonable agreement with published results for a total donor concentration of 10^{19} cm^{-3}.[3] The temperature run on the diffused layer was done to determine if the sulfur that was electrically inactive at room temperature might have been present in a complex with ionization energy larger than that of the shallow donor. No such center could be detected within the temperature range used. Optical methods may be needed if the center is very deep.[4]

Diffusions

Further diffusions have been done at $1215^{o}C$ to study the dependence of the sulfur surface concentration on sulfur pressure during diffusion. A new S-35 source has been used permitting the investigation of a much wider range of concentrations. The profiles are shown in Fig. 3, and a plot of surface concentration versus sulfur vapor density (proportional to P_{S_2}) is shown in Fig. 4 for these profiles, as well as those reported last quarter.

The experimental evidence suggests

$$\text{surface concentration} \propto (P_{S_2})^n \quad 1 < n < 1.5 \quad .$$

If n = 1, it is possible to invoke various complexes, admittedly somewhat artificial, that produce the correct dependence of concentration on pressure, e.g., $[V_{ga} - S_p - V_{ga} - S_p]$, $[S_{ga} - S_p]$ - a nearest neighbor substitutional pair, or $[S_i - S_i]$ - an interstitial pair. Yet to be answered are: objections concerning the plausibility of such complexes with respect to probability of formation, physical size and electron bonding.

A marked difference exists between doping from solution and from a vapor phase. In Trumbore's work[5]

$$\text{solubility} \propto (X_{s,melt})^n \qquad 1/2 < n < 1$$
$$\propto (P_{s_2})^k \qquad 1/4 < k < 1/2$$

whereas we observe

$$\text{solubility} \propto (P_{s_2})^m \qquad 1 < m < 1.5 \quad .$$

This suggests different incorporation mechanisms are operative for the 2 processes - at least one of which may then be a "non-equilibrium" one.

It has been assumed that the surface concentration in the diffusion profiles is the equilibrium solubility. The possiblity of precipitation should also be considered.

REFERENCES

1. T. Hara and I, Akasaki, J. Appl. Phys., 39, 285 (1968).
2. A. S. Epstein, J. Phys. Chem. Solids, 27, 1611 (1966).
3. H. C. Montgomery and W. L. Feldmann, J. Appl. Phys., 36, 3228 (1965).

4. L. J. Vieland and I. Kudman, J. Phys. Chem. Solids, 24, 437 (1963).

5. F. A. Trumbore, et al, J. Electrochem. Soc., 112, 782 (1965).

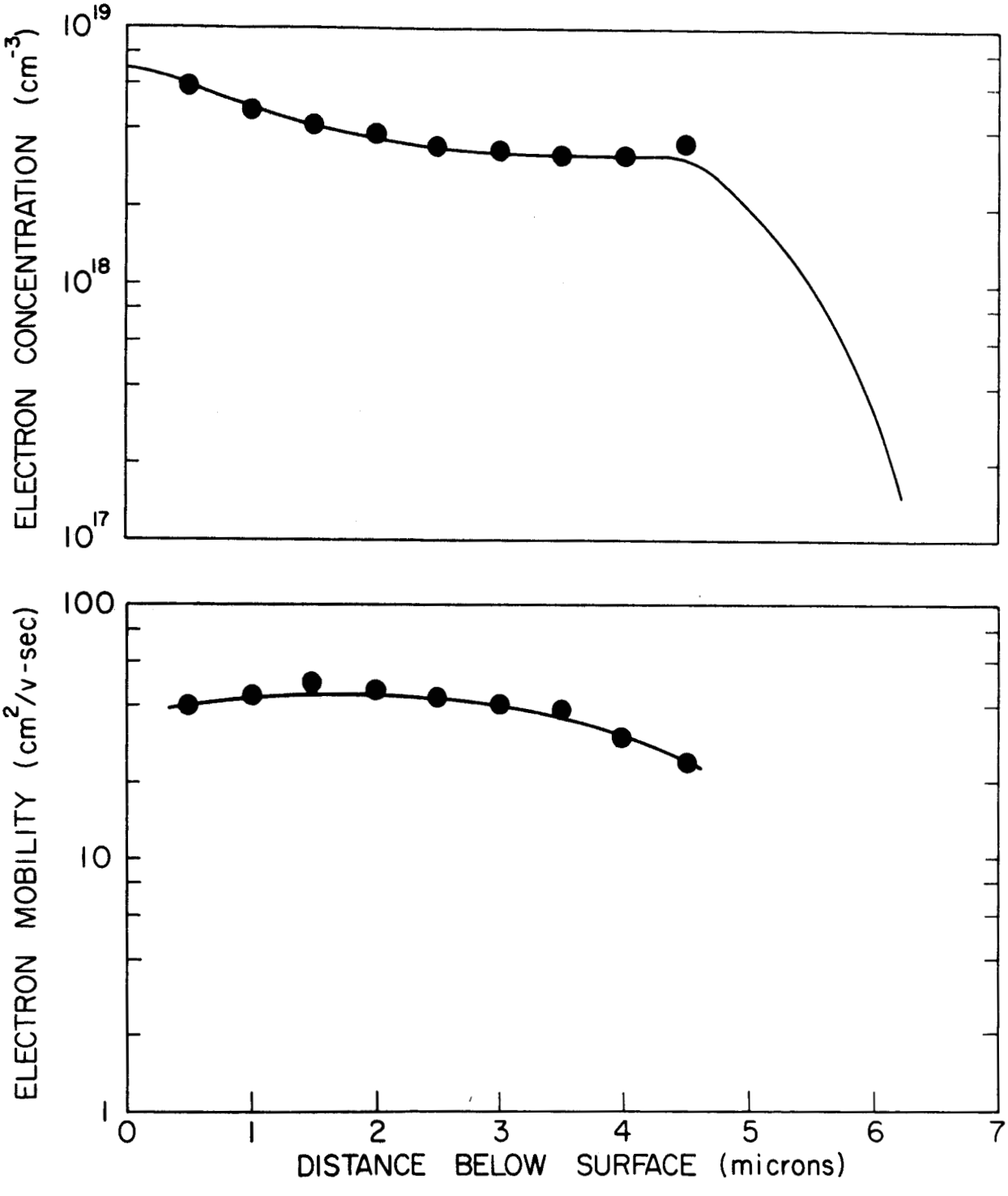

FIG. 1 - Electron concentration and mobility in sulfur - diffused layer (diffused through SiO_2 film).

B440

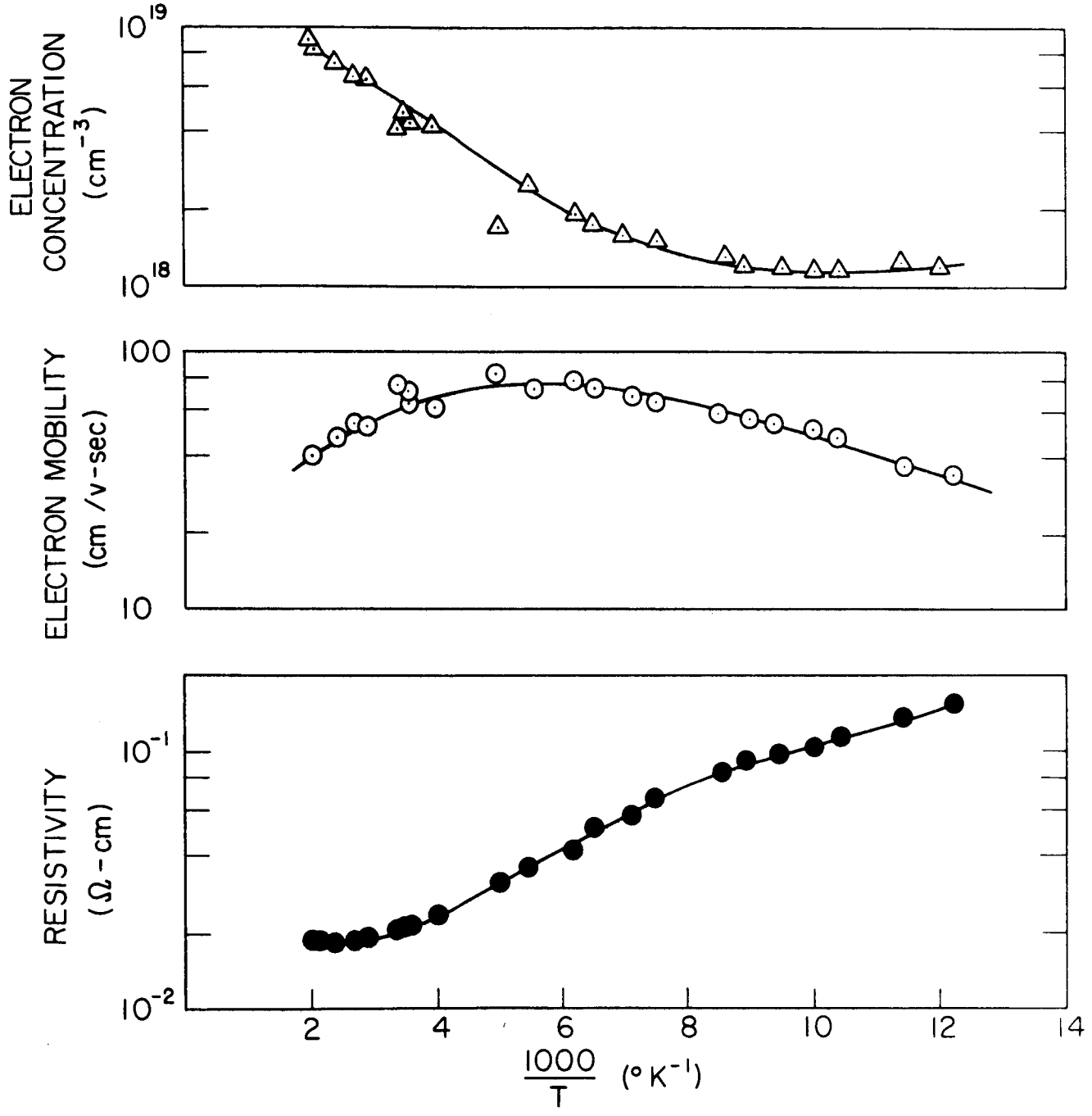

FIG. 2 - Electron concentration, mobility and resistivity in sulfur - diffused layer as a function of temperature.

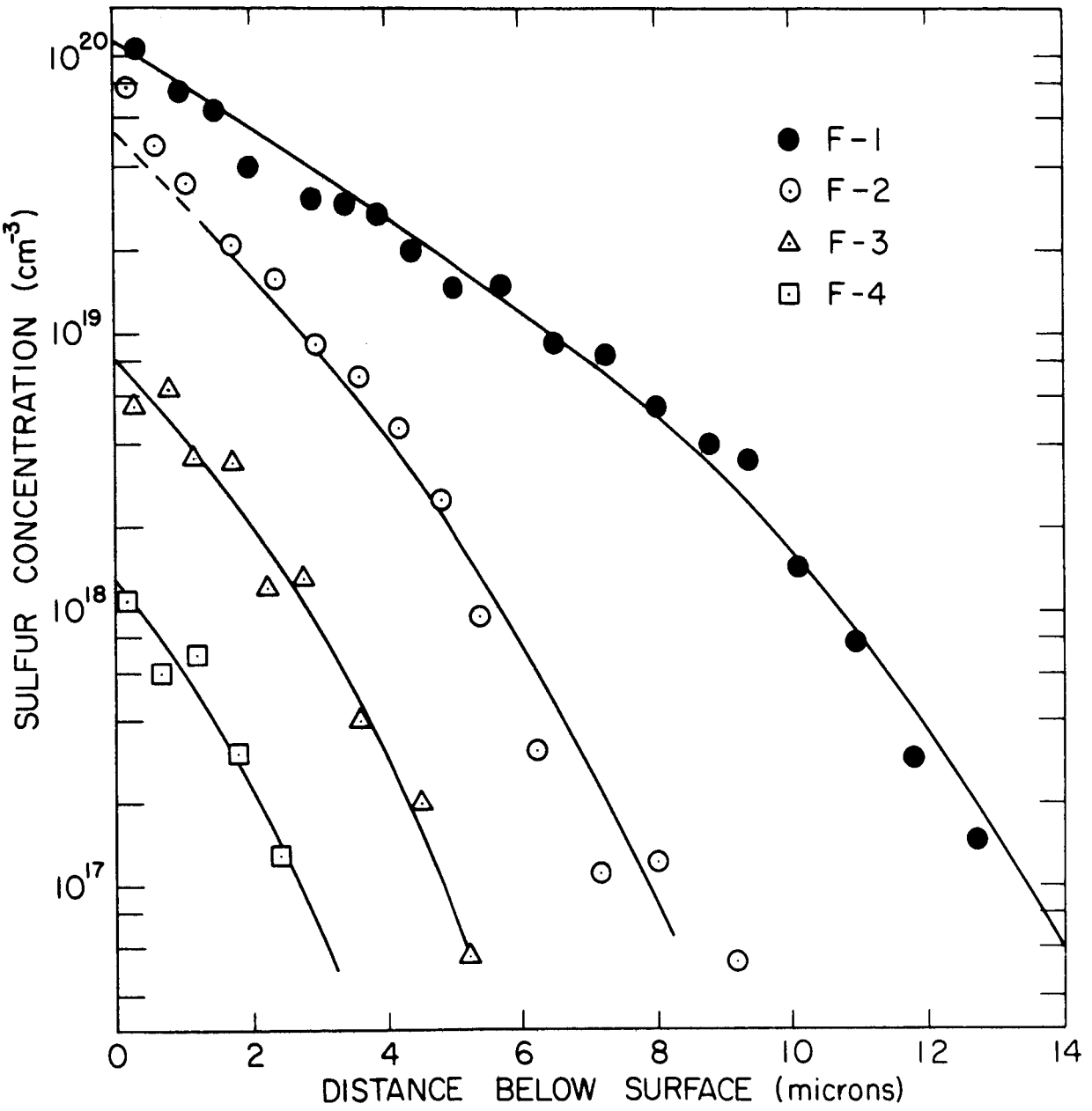

FIG. 3 - Variation of sulfur diffusion profiles in GaP as a function of sulfur pressure. (T = 1215°C, t = 12 hrs, [P] = 2 mg/ml; [S] = 6.5 μg/ml - F-1; 2 μg - F-2; 0.65 μg/ml - F-3; 0.2 μg/ml - F-4).

AN4089

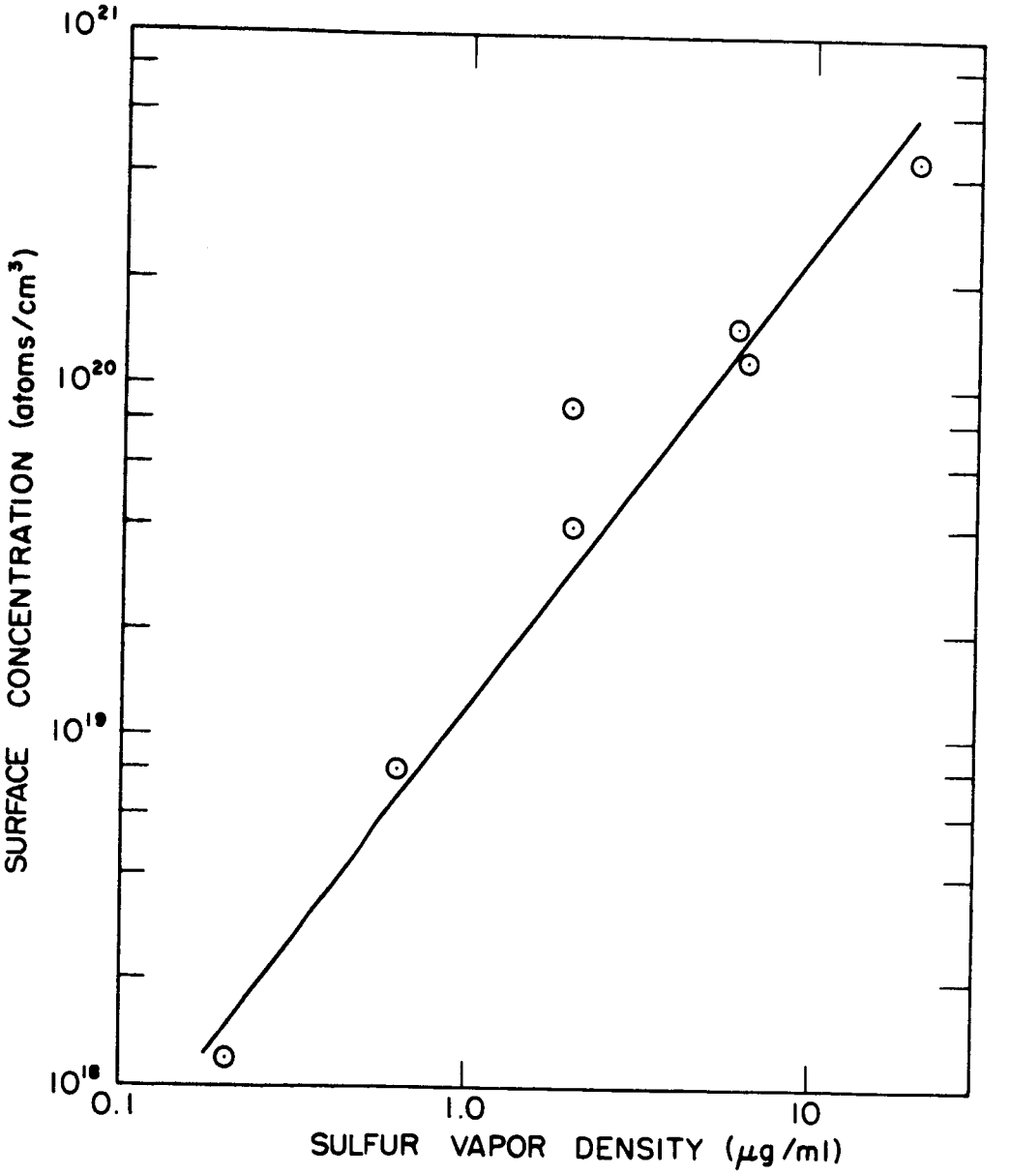

FIG. 4 - Variation of Surface Concentration as a function of sulfur pressure during diffusion (T = 1215°C).

A44088